J. Fluid Mech. (1993), *vol.* 250, *pp.* 277–305

Mixing by a turbulent plume in a confined stratified region

By SILVANA S. S. CARDOSO AND ANDREW W. WOODS

Institute of Theoretical Geophysics, Department of Applied Mathematics and Theoretical Physics, University of Cambridge, Silver Street, Cambridge CB3 9EW, UK

(Received 14 July 1992 and in revised form 23 November 1992)

An experimental and theoretical study of the mixing produced by a plume rising in a confined stratified environment is presented. As a result of the pre-existing stable stratification, the plume penetrates only part way into the region; at an intermediate level it intrudes laterally forming a horizontal layer. As time evolves, this layer of mixed fluid is observed to increase in thickness. The bottom front advects downward in a way analogous to the first front in the filling box of Baines & Turner (1969), while the lateral spreading of the plume occurs at an ever-increasing level and an ascending top front results. We develop a model of this *stratified filling box*; the model predicts the rate at which the two fronts advance into the environment.

It is found that stratification in the environment, when smooth, has no significant influence on the dynamics of the descending front. We show that the rate of rise of the ascending front is determined by the turbulent mixing occurring at the spreading level. Entrainment of environmental fluid from above into the overshooting plume is significant; as a result, a density interface develops at this level. Asymptotically, the system reaches a state in which a bottom convecting layer, with an almost homogeneous density, deepens in a stratified background. The model proposed for this large-time behaviour is based on the simple energetic formulation that a constant fraction of the kinetic energy supplied by the plume, for mixing across the interface, is converted into potential energy of the convective layer. Our experimental results suggest an efficiency of approximately 50% for this conversion.

We discuss our results in the light of previous studies on turbulent penetrative convection and conclude that the theory developed should be valid for an intermediate range of values of the Richardson number characterizing the dynamic conditions at the interface. The model is applied quantitatively to the process of cooling of a room wherein stratification is relevant. The geological problem of replenishment of a magma chamber by a light input of magma is also analysed.

1. Introduction

The effect of continuous convection from small sources of buoyancy on the properties of an environment of finite extent was first analysed by Baines & Turner (1969). They considered the situation in which the environment is initially uniform in density. An illustration of their problem is given in figure 1(*a*). The point source, located at the bottom of the bounded region, generates a plume of turbulent buoyant fluid rising under gravity. As the first fluid reaches the top of the closed space, it spreads out laterally and produces a layer with a density discontinuity below it – the first front. This layer is lighter than the original environment, and the continuing plume, which entrains fluid below the front, causes it to move down. Thus, new plume fluid will

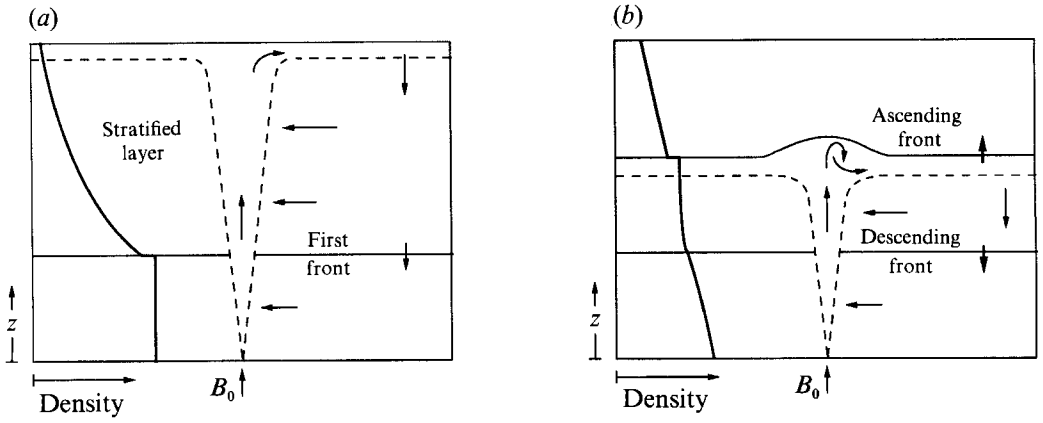

FIGURE 1. The different flow patterns induced by a plume rising in a confined region of large aspect ratio: (*a*) uniform environment (studied by Baines & Turner 1969); (*b*) linearly stratified environment (present work).

arrive at the top even lighter and a stable density distribution is built up, gradually filling the original uniform environment.

Baines & Turner (1969) proposed a detailed filling-box model for this interaction between the buoyant plume and the environment, taking into account the dependence upon time and space. Expressions for the position of the first front as a function of time and for the large-time density distribution in the environment were obtained. Laboratory experiments confirmed their predictions. Later, Worster & Huppert (1983) suggested an approximate analytic expression for the time-dependent density profiles in the developing stratification. The evolution of the density field at times for which the asymptotic solution of Baines & Turner is not applicable, had previously been followed numerically by Germeles (1975). The filling-box model was successful in giving a physical explanation for the counter-gradient buoyancy (or heat) flux observed in the atmosphere and oceanographic convective layers, and also in laboratory experiments on parallel plate convection. Earlier work, developed in terms of mean density distributions and a steady state, was incapable of explaining this phenomenon. The model was also applied to the process of cooling/heating a room, describing the way in which air mixes in such situations.

Manins (1979) extended the filling-box model, analysing the conditions that ensure that the source of buoyant convection is the dominant transport mechanism in the region. Restrictions on the aspect ratio (width/height) of the region and on the relative strength of the source were imposed. The manner in which the convective fluid recirculates to become part of the passive interior was studied in detail. Following this line of research, Barnett (1991) recently investigated, in the laboratory, the effect of the geometry of the region on the flow pattern. The filling-box process is observed to occur only for large aspect ratios. For moderate aspect ratios, a large-scale vertical circulation with overturning motion is set up and the environment becomes horizontally inhomogeneous. At the extreme of very small aspect ratios the flow becomes more complicated. At some distance from the source, the plume interacts with the wall and is unable to supply the return flow; the plume flow breaks down and thorough mixing with ambient fluid occurs. Unstable stratification then develops at this level, giving rise to turbulent convection further from the source.

Baines (1975) and Kumagai (1984) also extended the work of Baines & Turner, replacing the rigid upper boundary of the region by an overlying layer of light fluid.

They permitted entrainment of this fluid as the plume overshoots and penetrates the layer above. By including a moving density interface, more realistic modelling of geophysical problems was possible.

In the present work we shall analyse the situation in which the bounded environment, of large aspect ratio, is initially stably stratified. This is of interest since many geophysical processes involving mixing are often complicated by density stratification; thermal stratification in lakes or reservoirs, and salinity gradients in estuaries are common. This internal structure has a great effect on the flow pattern and associated hydrodynamic mixing.

When buoyant fluid is released in a stably stratified environment, the convective plume might not rise to the top of the region. Instead, as a result of the entrainment of relatively heavy fluid at the base of the closed space, the plume may come to a height where its density equals that of the surrounding fluid; it will then intrude sideways. The filling-box process will then occur on a different length and time scale from that in a uniform environment. The environment below the front of plume fluid descending towards the source will now be stratified, and there is no closed boundary at the top of the region (figure 1*b*). In this paper we analyse the dynamics of the mixing process induced by the plume under these conditions.

A series of laboratory experiments was performed to investigate the filling-box process in an initially linearly stratified ambient. Theoretical ideas are developed in the light of these experimental results. We study the effect of the changing stratification on the rate at which the descending front travels and compare our results with those obtained by Baines & Turner for a uniform environment. The evolution of the intruding level of the plume is analysed. We explore the implication of turbulent mixing between the plume and ambient fluids at the spreading level. A model, valid for large times and based on a simple energetic formulation, is developed.

The paper is organized as follows. In §2, we give a physical description of the problem and report qualitatively upon some laboratory experiments. In §3, the laboratory experiments are described. The theoretical model is developed in §4, and the theoretical ideas are investigated and compared with experimental results. In §5, we discuss the implications of our results with regard to the energetics of mixing processes in stratified environments. The relation with previous research on turbulent penetrative convection is analysed. Finally, the quantitative application of the model to two physical problems is described. The main conclusions of the work are summarized in §6.

2. A physical description

Consider a small continuous source of buoyancy in a confined region which is initially stably stratified. This may be achieved in the laboratory by injecting, for example, water through a small nozzle placed at the bottom of a tank containing a stratified salt solution. The resulting flow pattern is demonstrated by the sequence of laboratory photographs shown in figure 2. The plume fluid has been dyed for visualization.

The light convecting fluid forms a turbulent plume which entrains dense surrounding fluid as it rises. The plume density will thus increase steadily with height, while that of the environment decreases steadily. At some level the density difference will vanish, although excess momentum causes the plume to continue rising. Ultimately the negative buoyancy forces on the plume bring it to rest, and the fluid in the topmost part of the plume falls back some distance as it spreads out sideways to form a horizontal

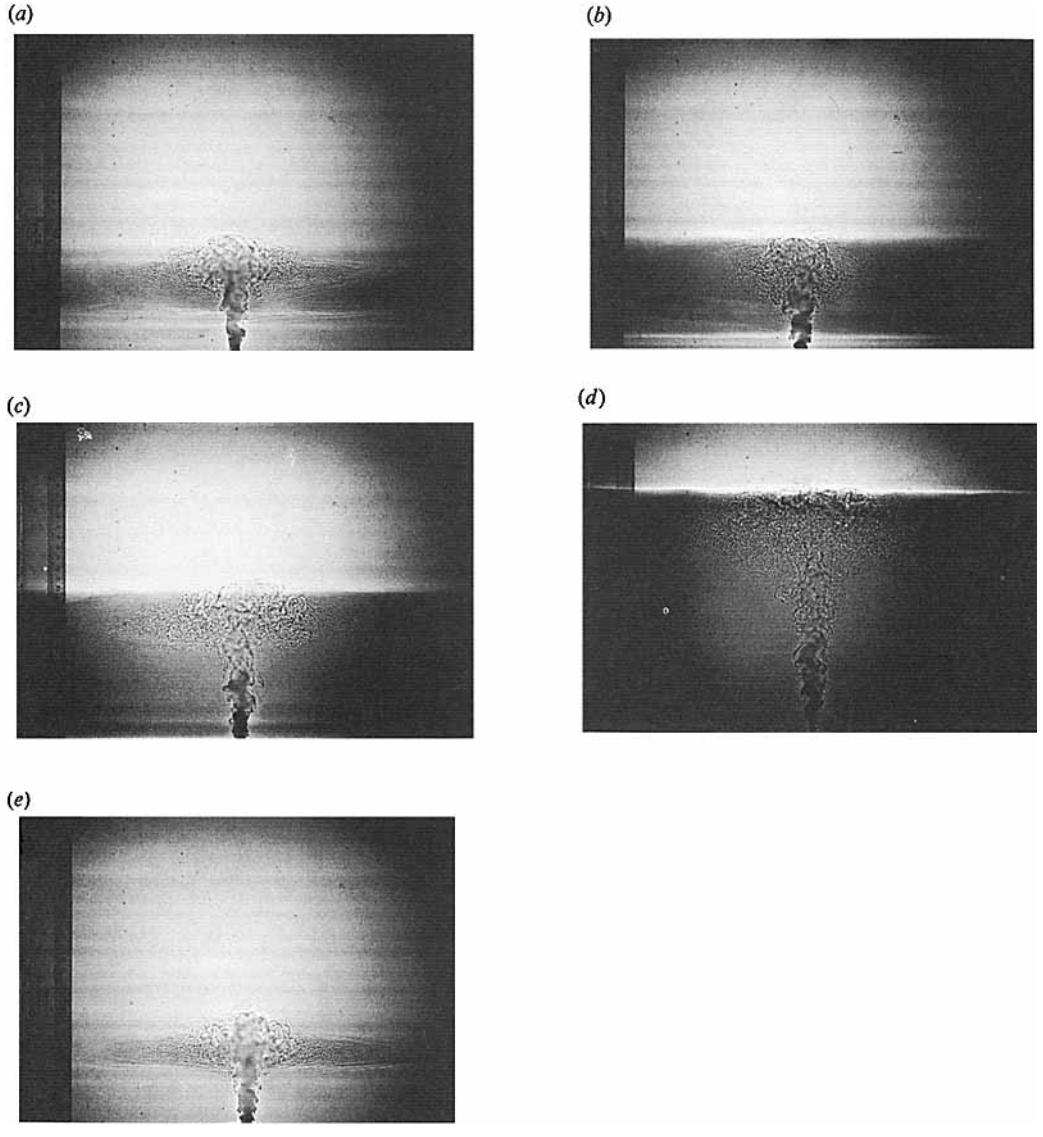

FIGURE 2. Evolution of the convective process induced by a plume rising in a linearly stratified environment of finite lateral extent. The plume fluid has been dyed for visualization. The photographs are of experiment 7A at times (*a*) 1.5 min, (*b*) 5 min, (*c*) 15 min, (*d*) 36 min and (*e*) 120 min. (The photographs are actually inverted for consistent nomenclature of fronts.)

layer. The height at which this occurs lies between the level of neutral buoyancy and that where the vertical velocity vanishes. This inertial overshoot and the spreading intrusion can be seen in figure 2(*a*). As a result of the continual removal of ambient fluid by entrainment into the plume, there will be a downward flow of that fluid. Hence a front of the fluid that has been in the plume descends, analogous to the first front of Baines & Turner (1969).

As time evolves, the density field in the environment changes. In the region below the top of the plume the density gradient is sharpened due to differential entrainment, and at the same time buoyancy increases. These two changes have opposing effects on the resistance to the rise of the plume. Let us examine the evolution of the system shown

Expt	B_0 (cm^4 s^{-3})	N (s^{-1})	A_0 (cm s^{-2})	Injection	Symbol
1A	67	1.66	89	bottom	●
2A	91	1.62	124	top	■
3A	61	1.06	77	bottom	▲
4A	39	0.956	45	bottom	◆
5A	93	0.672	157	top	+
6A	60	0.677	30	bottom	○
7A	65	1.05	124	top	□
1B	41	0.634	46	bottom	△
2B	65	0.867	73	bottom	◇
3B	67	1.32	103	top	⊕

TABLE 1. The experimental conditions. Labels A and B refer to the tank used (see §3).

in figure 2. It is clearly seen that the top front of plume fluid is rising. The increase in buoyancy then seems to be the predominant effect. The upper part of the plume is now surrounded by, and thus entrains, lighter fluid. The buoyancy forces in the plume experience a smaller resistance and so the plume will spread out at an ever-increasing level. We shall see later that this result is independent of the particular input conditions of the experiment.

In this way two fronts develop in the environment, separating fluid which has at some time been in the plume from the original tank fluid; one moves upwards while the other is moving down towards the source. In §4, we present a theoretical model of this mixing and predict the rate at which the two fronts advance into the environment. We shall now describe the experimental method.

3. The experiments

The experiment consists of releasing buoyant fluid, at a steady rate, through a small nozzle into a tank of fluid in which there is a stable linear density variation. The stratification was produced with salt solution, using the double bucket system (Oster 1965). The experiments were carried out in two rectangular tanks differing in cross-sectional area. Tank A is glass-walled, 57.7×42.8 cm in cross-section and 44 cm deep; tank B is made of Perspex, has 24.9×25.0 cm cross-section and 30 cm depth.

The source fluid used was either water or a dense salt solution. It was supplied through a 7 mm diameter nozzle placed either at the free surface or at the bottom of the tank, for negative and positively buoyant releases respectively. A flowmeter was used to control the rate of addition of fluid. The flow rates used were sufficiently small for the source to approximate one of buoyancy alone and the mass flux could be ignored. The liquid released was dyed with food colouring so that its motion could be observed. A shadowgraph technique was used to follow changes in position of the top and bottom fronts of plume fluid.

The density distribution in the tank was determined by withdrawing small samples of fluid, typically 1 ml, at different levels with a syringe. The density was measured by refractometry.

Experiments were carried out with buoyancy fluxes at the source ranging from 39 to 93 cm^4 s^{-3}; the buoyancy frequency of the initial stratification was varied from 0.634 to 1.66 s^{-1}. The plume appeared to be fully turbulent and the Reynolds number was of the order of 2×10^3. Table 1 summarizes the experimental conditions for each run. The symbols are those used in figures 3, 5 and 8.

The position of the virtual source was determined by the method suggested in Baines & Turner (1969). The entrainment coefficient, α, was approximately 0.09, which is in accord with the value reported in the extensive work on turbulent plumes by Papanicolaou & List (1988). The resulting length corrections (~ 1 cm) agree with the theoretical predictions obtained assuming that the bounding surface of the plume passes through the edge of the nozzle (Morton, Taylor & Turner 1956).

4. The theoretical model

Consider a stably stratified region which is horizontally limited, say of uniform cross-sectional area $A = \pi R^2$, where R is an equivalent radius. We assume that a plume rises through this region and spreads out at height H_s. Owing to the continuous variation of the ambient properties described above, the behaviour of the plume is time-dependent. However, if the aspect ratio R/H_s is large, for all times and heights, then the time rates of change of the plume properties can be shown to be sufficiently small to be neglected in the relevant conservation equations (Manins 1979). The plume is then of small radius, compared to R, and the ambient behaves quasi-steadily as far as the plume is concerned.

Using the Boussinesq approximation and assuming a constant coefficient of entrainment, the equations representing conservation of volume, momentum and buoyancy for a plume issuing from a point source of buoyancy, are respectively (Morton *et al.* 1956)

$$\frac{\mathrm{d}}{\mathrm{d}z}(a^2\omega) = 2\alpha a\omega, \quad \frac{\mathrm{d}}{\mathrm{d}z}\left(\frac{a^2\omega^2}{2}\right) = a^2 \Delta, \quad \frac{\mathrm{d}}{\mathrm{d}z}\left(\frac{a^2\omega\Delta}{2}\right) = a^2\omega\frac{\partial \Delta_e}{\partial z}. \tag{4.1a–c}$$

Here z denotes a space coordinate, increasing upward, with its origin at the point source; a is the effective radius of the plume; ω is the vertical velocity at the plume axis; α is the entrainment coefficient; and Δ and Δ_e are, respectively, the buoyancy of the plume evaluated on the plume axis and the buoyancy in the environment, defined by

$$\Delta = g(\rho_e - \rho)/\rho_r, \tag{4.2}$$

$$\Delta_e = g(\rho_e - \rho_r)/\rho_r. \tag{4.3}$$

Here, g is the acceleration due to gravity; and ρ denotes density, ρ_r being a reference density. Gaussian profiles of equal width have been assumed for the vertical velocity and buoyancy distributions in the plume. Equations (4.1) were originally derived by Morton *et al.* (1956) and have been discussed in detail elsewhere (e.g. Turner 1979).

For the dynamics of the environment below the spreading height, we follow the filling-box model proposed by Baines & Turner (1969). It is assumed that the weak downward motion of the outside fluid, caused by entrainment into the plume, can be described by an average velocity U. This condition is verified more easily for strong stratifications and large aspect ratio R/H_s, the vertical velocity in the environment being then horizontally uniform. In this case two other relations will be satisfied in the region. With the Boussinesq approximation, conservation of mass may be written

$$-\pi R^2 U = \pi a^2 \omega \tag{4.4}$$

since $R^2 \gg a^2$, and the buoyancy field is governed by

$$\frac{\partial \Delta_e}{\partial t} = -U\frac{\partial \Delta_e}{\partial z}, \tag{4.5}$$

where molecular diffusion and mixing have been neglected.

The dynamics of the descending and ascending fronts are now considered in turn.

4.1. *The descending front*

As mentioned above, when a plume rises in a stable environment, it overshoots past the level of zero buoyancy. At the top it forms a fountain, falling back in an annular region surrounding the upflow and finally it spreads out horizontally. These observations suggest that there should be some degree of mixing between the fluid in the collapsing fountain and the environment. It is, in fact, known that the height at which this fluid flows out sideways lies slightly above the level at which the plume density first equals that of the environment (Turner 1979); this seems to be the result of some mixing. However, the entrainment of ambient fluid at the top of the plume does not affect the rate of advance of the front of buoyant fluid which first spreads out and begins to descend. The movement of the front is totally determined by the rate of entrainment into the plume from the region below, where original ambient fluid still exists.

The details of the lateral outflow are of secondary importance if the thickness of this region is small compared to H_s. The intrusion then spreads out quickly compared to the timescale of the vertical flow in the ambient (see Appendix A). We shall assume that the plume fluid spreads out instantaneously into a thin horizontal layer, at the neutral buoyancy height. In fact, the bottom of the actual spreading layer will lie close to this height (Turner 1986).

Equations (4.1) and (4.4)–(4.5) may now be solved for the rate of advance of the descending front. Let us introduce the non-dimensionalized variables

$$\left.\begin{aligned} \zeta = H^{-1}z, \quad \tau = 4\pi^{\frac{2}{3}}\alpha^{\frac{4}{3}}H^{\frac{2}{3}}A^{-1}B_0^{\frac{1}{3}}t, \quad \delta = 4\pi^{\frac{2}{3}}H^{\frac{5}{3}}B_0^{-\frac{2}{3}}\Delta_e, \\ j = \tfrac{1}{2}\pi B_0^{-1}a^2\omega\Delta, \quad q = \tfrac{1}{4}\pi^{\frac{1}{3}}\alpha^{-\frac{4}{3}}H^{-\frac{5}{3}}B_0^{-\frac{1}{3}}a^2\omega, \quad m = \tfrac{1}{2}\pi^{\frac{1}{3}}\alpha^{-\frac{1}{3}}H^{-\frac{2}{3}}B_0^{-\frac{1}{3}}a\omega, \end{aligned}\right\} \tag{4.6}$$

where

$$H = 2^{-\frac{7}{8}}\pi^{-\frac{1}{4}}\alpha^{-\frac{1}{2}}B_0^{\frac{1}{4}}N^{-\frac{3}{4}}, \tag{4.7}$$

B_0 is the buoyancy flux at the source and N is the buoyancy frequency in the original environment. H is proportional to the height at which the plume first spreads out; this lengthscale was originally introduced by Morton *et al.* (1956). For a plume in a stable linear stratification, the level of neutral buoyancy is at $\zeta = 2.13$ and the maximum height is at $\zeta = 2.8$ (Turner 1979).

The new dependent variables j, q and m^2 represent the fluxes in the plume of buoyancy, volume and momentum, and δ represents the buoyancy of the environment. The new independent variables ζ and τ are the non-dimensional height and time, respectively. In terms of these new variables, (4.1) may be written

$$\frac{\mathrm{d}q}{\mathrm{d}\zeta} = m, \quad \frac{\mathrm{d}m^4}{\mathrm{d}\zeta} = 2qj, \quad \frac{\mathrm{d}j}{\mathrm{d}\zeta} = q\frac{\partial\delta}{\partial\zeta}, \tag{4.8a–c}$$

while (4.4) and (4.5) may be combined to give

$$\frac{\partial\delta}{\partial\tau} = q\frac{\partial\delta}{\partial\zeta}. \tag{4.9}$$

The initial and boundary conditions required for unique solution of the governing equations are as follows. The initial condition is that the stratification in the environment is linear:

$$\delta = -2^{-\frac{1}{8}}\zeta \quad \text{at} \quad \tau = 0. \tag{4.10a}$$

The boundary conditions specify the plume fluxes of volume, momentum and buoyancy at the source:

$$\left.\begin{aligned} q = m = 0 \\ j = 1 \end{aligned}\right\} \quad \text{on} \quad \zeta = 0 \qquad \begin{aligned} &(4.10b, c) \\ &(4.10d) \end{aligned}$$

We have imposed one more continuity condition on the model: the plume spreads

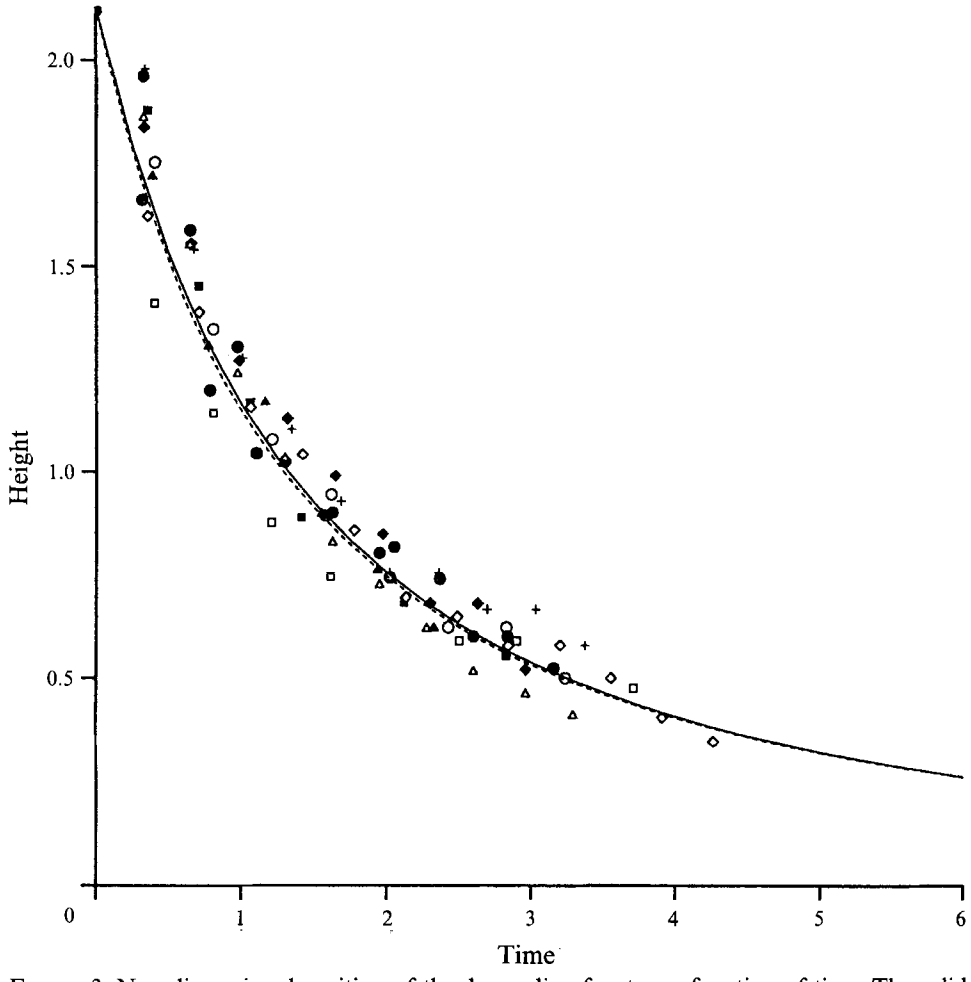

FIGURE 3. Non-dimensional position of the descending front as a function of time. The solid curve is the numerical solution of (4.8)–(4.10), for a linearly stratified environment. The dashed curve corresponds to the theory of Baines & Turner (1969), for a uniform environment. Symbols are experimental data (see table 1 for conditions).

out instantaneously at the neutral buoyancy height. The density of the environment at this level must therefore be equal to the average density of the liquid discharged by the plume,

$$j = 0 \quad \text{at the spreading height.} \tag{4.10e}$$

Equations (4.8) and (4.9) are in suitable form for numerical integration. The numerical scheme used is similar to that described by Germeles (1975); the initial step is carried out using an asymptotic power series solution, the leading terms of which equal those in a uniform surrounding (see e.g. Baines & Turner 1969). In this scheme the density of the environment is represented by a stepped profile. At each time step (4.8*c*) is integrated analytically to give the corresponding stepped profile for j, while (4.8*a*, *b*) are integrated numerically by a Runge–Kutta integrating scheme. Finally, the method of characteristics applied to (4.9) determines how the density levels move with time.

The result of the numerical integration is shown graphically in figure 3. Experimental data on the position of the first front as a function of time have also been plotted. It is seen that the agreement is good.

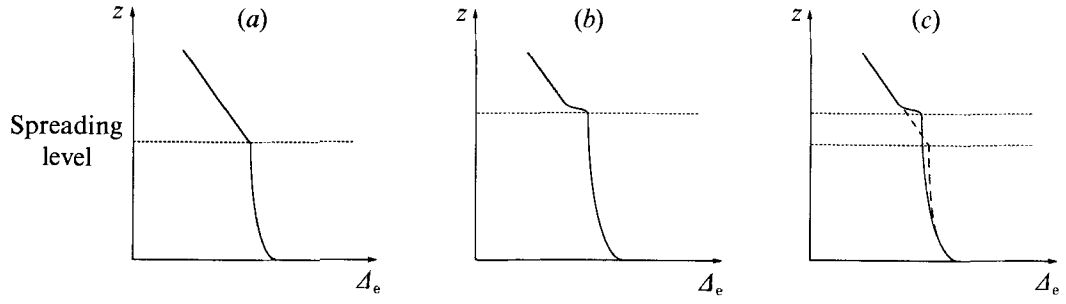

FIGURE 4. A schematic of the distribution of density in the environment at the spreading level of the plume for (*a*) and encroachment process, (*b*) an entrainment process and (*c*) comparison between (*a*) and (*b*).

It is interesting to compare these results with those obtained in a uniform environment. The dimensionless position of the front in this latter case is given by (Baines & Turner 1969)

$$\tau = 5(\tfrac{5}{18})^{\frac{1}{3}}(\zeta^{-\frac{2}{3}} - 2.13^{-\frac{2}{3}}), \tag{4.11}$$

which is represented in figure 3 as a dashed line. It is seen that the two curves differ very little, in fact by less than 4% (for a fixed height). This means that the fronts in uniform and in initially linearly stratified media travel almost equally fast. The behaviour of the plume in the developing stratification must then be very similar to that in a uniform environment. This is not so surprising when one recalls that the behaviour of a plume in a linearly stratified environment is only a little different from that in a neutral environment, almost up to the spreading height (Turner 1979).

The difference observed in figure 3 is small because the ambient stratification is smooth (the buoyancy profiles will be analysed in the next section). Only when the buoyancy profile has a strong gradient some distance away from the source will entrainment be significantly reduced and the descending front hindered. Indeed, Baines & Turner (1969) reported that for large times, when an 'asymptotic density' gradient had developed in their system, fronts travelled approximately 11% slower than the first front, for which the environment was uniform in density.

However, if the environment is smoothly stratified in the region above the source (although it may have a sharp variation in buoyancy very close to the source), the relation between the position of the front ζ and the time τ at which this is attained will be well predicted by (4.11), with time measured from the moment the plume first spreads out.

We thus conclude that stratification, when smooth, has no significant influence upon the filling-box timescale, other than determining the height at which the plume first spreads out.

4.2. *The ascending front*

We have seen that the level at which the plume spreads out laterally increases with time due to the increase in buoyancy of the surrounding environment. The rate at which this front of fluid rises will clearly depend on turbulent mixing at the top of the plume. However, if this effect is negligible, the process of rise will be one of simple *encroachment*; the upward rising plume fluid continuously erodes the stable stratification above, since it ascends further as the environmental buoyancy increases (figure 4*a*). On the other hand, significant mixing between the upper surface of the plume and the ambient fluid will result not only in entrainment of ambient fluid from above into the plume, but will also affect the density distribution in some region above

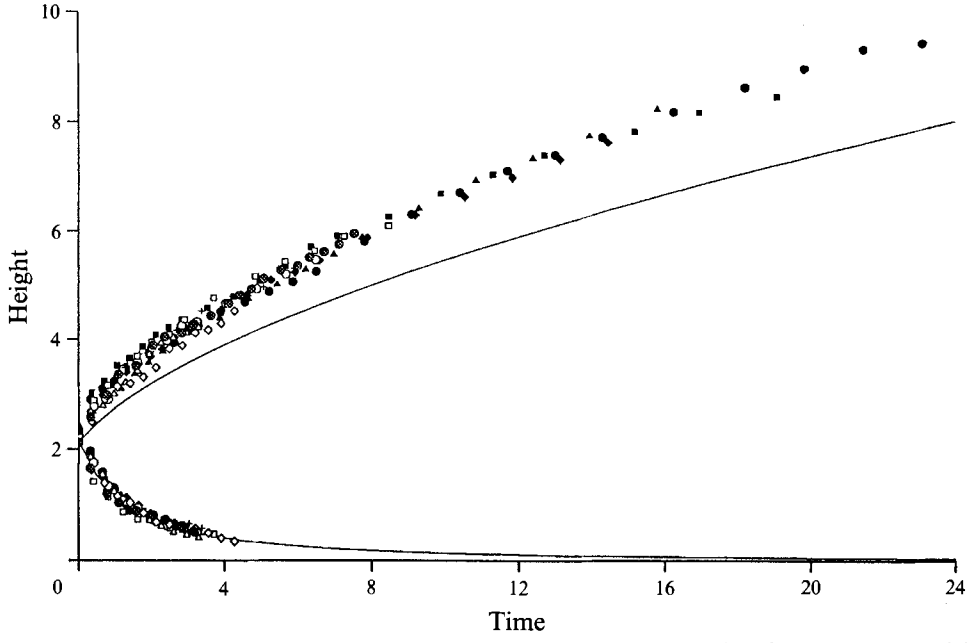

FIGURE 5. Evolution of the non-dimensional position of the ascending front as predicted by the encroachment model. The results for the descending front (obtained above) are also shown.

the spreading height (figure 4*b*). The continuing plume will then rise to a height that is strongly determined by the new buoyancy profile in this region. We note that the encroachment mechanism only occurs as a result of the finite lateral extent of the region; in an infinite medium it could not occur. In contrast, turbulent mixing and associated entrainment are intrinsic processes, independent of the extent of the region.

We shall now develop a model for the rate of rise of the ascending front. We begin by analysing the role of entrainment at the top of the turning plume.

4.2.1. *The encroachment model: negligible turbulent mixing at the spreading level*

Consider the simple limiting situation in which turbulent mixing at the top of the plume is negligible. In this case we can assume that there is no entrainment of fluid from above and the spreading height will thus coincide with the neutral buoyancy height.

The equations describing this situation are the same as considered previously and in non-dimensional form reduce to (4.8)–(4.10). The predicted evolution of the neutral buoyancy height as a function of time is plotted in figure 5. Comparison with experimental results shows that this model underpredicts the rate of rise of the spreading height by about 20%. This seems to indicate that entrainment of ambient fluid during the inertial overshoot of the plume is significant.

At this stage it becomes important to analyse the evolution of the buoyancy distribution in the environment. In figure 6 we present the model predictions for the buoyancy profile at different times together with our experimental data.

For small times the agreement between theory and experiment is relatively good. However, for larger times the difference becomes significant. Below the height at which the buoyancy equals that of the initial linear profile, theory slightly underestimates the actual decrease of buoyancy in the environment. Above this height, the model predicts that the buoyancy is unchanged and hence the initial stratification is preserved; in the

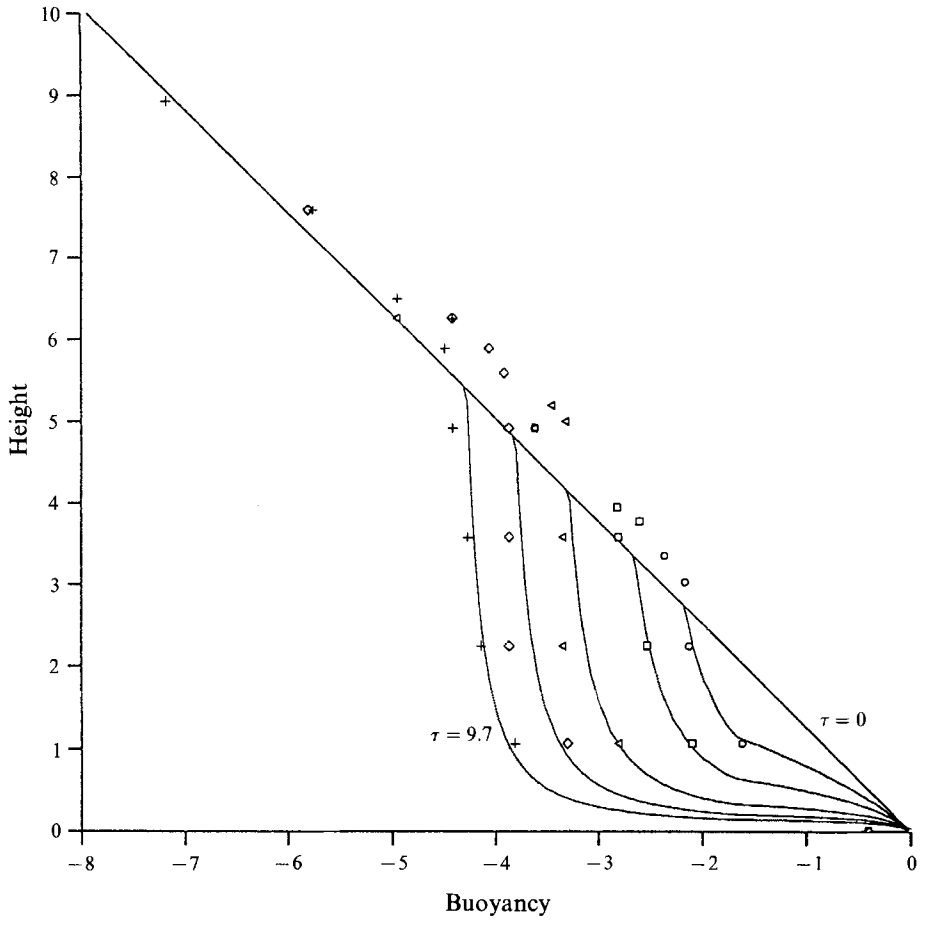

FIGURE 6. The buoyancy profile in the environment, Δ_e, at times $\tau = 0$, 1.0, 2.4, 4.8, 7.3 and 9.7. The curves represent the prediction of the encroachment model. The data are from experiment 7A. Note the increase in stratification below the descending front as a result of differential entrainment.

region just above the theoretical position of the interface, the experimental results show that the buoyancy is actually larger than the value in the initial stratification, as expected for conservation of buoyancy. The filling-box region is actually deeper and the density gradient at its top is greater than predicted by the encroachment model. These observations suggest that a significant amount of turbulent mixing with the environment occurs at the top of the plume. Owing to limitations of the experimental technique used, it was not possible to obtain a more detailed description of the buoyancy profile near the spreading level. Nevertheless, it seems clear that there is indeed some entrainment at the upper surface of the plume and it is this that we wish to show.

4.2.2. *A well-mixed model for large times*

Returning to figure 6, it is important to draw attention to the shape of the density profiles at large times. Apart from a thin region near the source, the buoyancy distribution in the environment is almost uniform. This is because the timescale over which the ascending front rises is very much longer than the timescale over which environmental fluid is recirculated through the plume (the filling-box time). Thus, at times larger than the filling-box timescale, the environment surrounding the plume is

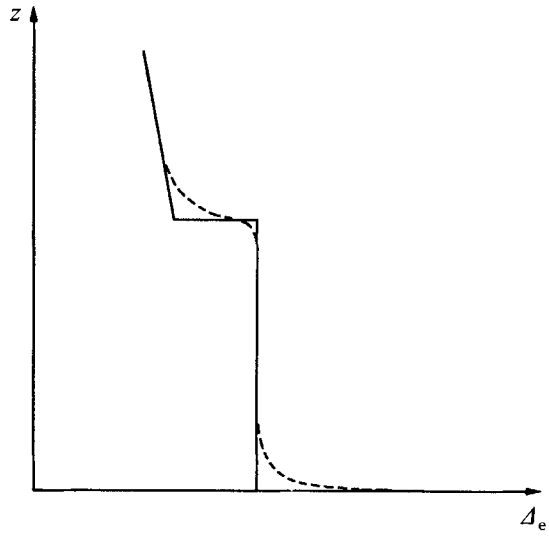

FIGURE 7. A schematic of the real buoyancy profile in the environment at large times (dashed line) and corresponding approximation of the well-mixed model (solid line).

approximately well-mixed. In the region where the plume is spreading out, a density interface develops as a result of the entrainment. The buoyancy difference is localized in a thin layer, while the fluid above preserves the initial stratification.

For times larger than the filling-box time we can, therefore, adopt a simple model, in which the vertical density profile is approximated by a discontinuous function:

$$\Delta_e = \begin{cases} \bar{b}, & z < h \\ \bar{b} - \Delta b - N^2(z-h), & z > h, \end{cases} \tag{4.12}$$

where $\bar{b}$ is the mean value of the buoyancy in the convective layer and Δb represents the buoyancy difference at the interface. A representation of schematic and realistic profiles of $\Delta_e(z)$ is shown in figure 7.

Let us consider the process of mixing across this density interface. Whenever fluid immediately above the interface is entrained, it is displaced vertically from its equilibrium position: light fluid is transported down into a layer of heavy fluid against the restoring buoyancy force. Work must be done to overcome this resistance, and this work is supplied by the agent causing the mixing – the plume.

We can thus understand that the rate of growth of the mixed layer in the background of a stable stratification will be strongly restricted. A considerable part of the kinetic energy supplied by the plume to the top of the convective layer will be used in overcoming the buoyancy forces required to entrain fluid from above. It is the resulting interactive evolution of the convective layer depth, h, and the buoyancy jump at the interface, Δb, that we wish to analyse.

The kinetic energy flux associated with the mean flow in a plume rising in a uniform environment is given by

$$E_{K_m} = \int_0^{+\infty} \rho\omega(r)\frac{\omega^2(r)}{2} 2\pi r \, dr. \tag{4.13}$$

Performing the integration for a Gaussian profile of velocity (see e.g. Turner 1979) and using the Boussinesq approximation, leads to

$$E_{K_m} = \tfrac{1}{6}\rho_r \pi a^2 \omega^3 = \tfrac{1}{2}\rho_r B_0 h, \tag{4.14}$$

where h is the height considered. The kinetic energy flux associated with turbulence can be shown to be small, less than 7% of that of the mean flow (see Appendix B). We will therefore consider, as in classical plume theory, that the turbulent energy flux is negligible. The kinetic energy supplied by the plume to the top of the mixed layer is then given by (4.14).

It is now necessary to evaluate the rate of work for entrainment. The volume rate at which light fluid is entrained at the interface is $(\mathrm{d}h/\mathrm{d}t)A$; this fluid is distributed uniformly through the whole depth of the convective layer. Its centre of mass will thus descend a distance $\frac{1}{2}h$, with the work involved in the process being

$$W = \rho_r \Delta b \frac{h}{2} \frac{\mathrm{d}h}{\mathrm{d}t} A. \tag{4.15}$$

This expression represents the rate of increase of potential energy of the mixed layer due to entrainment at the interface. As an alternative, in Appendix C, we derive (4.15) from energetic considerations.

If we assume that the work done per unit time is proportional to the rate of input of kinetic energy at the interface, then

$$\rho_r \Delta b \frac{h}{2} \frac{\mathrm{d}h}{\mathrm{d}t} A = \tfrac{1}{2} f \rho_r B_0 h, \tag{4.16}$$

where f is a dimensionless constant indicating the fraction of kinetic energy converted to potential energy of the mixed layer.

Conservation of buoyancy over the well-mixed region requires that

$$(\mathrm{d}/\mathrm{d}t)(\tfrac{1}{2}N^2h^2 - h\Delta b) = B_0/A. \tag{4.17}$$

We may now use (4.16) and (4.17) to determine h and Δb for a prescribed buoyancy flux at the source, B_0, and a prescribed buoyancy frequency, N, in the undisturbed region.

The particular initial conditions for this problem, h_0 and Δb_0 at $t = 0$, are not relevant. The model developed above is only valid for large times when h and Δb have lost their dependence on peculiarities of their behaviour in the initial period. Let us begin by taking

$$h_0 = \Delta b_0 = 0. \tag{4.18a, b}$$

Introducing the scale for the buoyancy jump at the interface to be $\frac{1}{2}N^2H$, leads to the non-dimensional variable

$$\Delta\beta = 2\Delta b/N^2H. \tag{4.19}$$

The non-dimensional variables for time, τ, and length, ζ, have been defined in (4.6). Equations (4.16), (4.17) and the initial conditions (4.18) now take the dimensionless form

$$(\mathrm{d}/\mathrm{d}\tau)(\zeta^2 - \Delta\beta\zeta) = 2^{\frac{4}{3}}, \tag{4.20}$$

$$\Delta\beta\, \mathrm{d}\zeta/\mathrm{d}\tau = 2^{\frac{4}{3}} f, \tag{4.21}$$

$$\zeta_0 = \Delta\beta_0 = 0. \tag{4.22a, b}$$

Integration gives the evolution of the convective layer depth and buoyancy jump at the interface

$$\zeta = 2^{\frac{2}{3}}((1+2f)\tau)^{\frac{1}{2}}, \quad \Delta\beta = \frac{2f}{1+2f}\zeta. \tag{4.23a, b}$$

It is now interesting to compare these theoretical predictions with our experimental results. However, we cannot use the solutions in (4.23) directly, because in our experiments the buoyancy flux at the source relative to the environment is decreasing with time. Indeed, the buoyancy of the convective layer continuously increases as a result of both the injection of buoyancy at the source and entrainment at its top boundary; the behaviour of the plume in this uniform environment therefore also varies. This will affect the flux of kinetic energy supplied by the plume to the density interface; a time-dependent correction should be introduced in (4.14). We derive this modification below.

Modification of model for a variable buoyancy flux relative to the environment

The parameter defining the behaviour of a plume arising from a point source of buoyancy in a uniform environment is the buoyancy flux, B_0. For the ideal point source, for which the volume flux Q_0 is zero, the buoyancy at the source Δ_0 is infinite ($B_0 = Q_0 \Delta_0$). Then, finite changes in the buoyancy of the environment, Δ_e, do not affect the plume behaviour since Δ_0 remains infinite when compared to Δ_e.

However, in the case of a real source, the buoyancy Δ_0 will be far from being infinite. If buoyancy is generated by heat, say a constant heat flux at the source, then even when Δ_e is changing in time, $\Delta_0 - \Delta_e$ will remain constant; hence, relative to the environment, B_0 will remain constant. However, if the source of buoyancy consists, for example, of a supply of fluid of constant density, then as Δ_e changes in time, $\Delta_0 - \Delta_e$ will also change; the relative strength of the source, expressed by the magnitude of the buoyancy flux, will be affected by changes in the buoyancy of the environment. The buoyancy flux at the source relative to the environment will now be given by

$$B_{0_r} = B_0 \frac{\Delta_0 - \Delta_e}{\Delta_0}, \tag{4.24}$$

where Δ_e has been taken as zero at $t = 0$. This correction is only necessary when considering plume properties that are defined relative to the environment. A similar effect of changing buoyancy has been analysed by Baines, Turner & Campbell (1990) in the different context of a turbulent dense fountain.

In our experiments, the changing buoyancy of the environment can be expressed in terms of the convective layer depth, h, and the buoyancy step at the interface, Δb, as

$$\Delta_e = N^2 h - \Delta b. \tag{4.25}$$

The rate at which kinetic energy is supplied by the plume is then (cf. (4.14))

$$E_{K_m} = \rho_r B_0 h \left(1 - \frac{N^2 h - \Delta b}{\Delta_0}\right). \tag{4.26}$$

The non-dimensional equations describing the evolution of the convective layer depth, ζ, and the buoyancy jump at the interface, $\Delta\beta$, now read

$$\frac{d}{d\tau}(\zeta^2 - \Delta\beta\zeta) = 2^{\frac{4}{3}}, \quad \Delta\beta \frac{d\zeta}{d\tau} = 2^{\frac{4}{3}} f\left(1 - \left(\frac{N^2 H}{\Delta_0}\right)(\zeta - \tfrac{1}{2}\Delta\beta)\right) \tag{4.27a, b}$$

(compare with (4.20) and (4.21)).

The value of the parameter $N^2 H/\Delta_0$ depends on the particular experiment. However, it differs little for the experiments described in §3, and the effect of this variation on the results is less than the scatter inherent to the experimental measurements (see Appendix

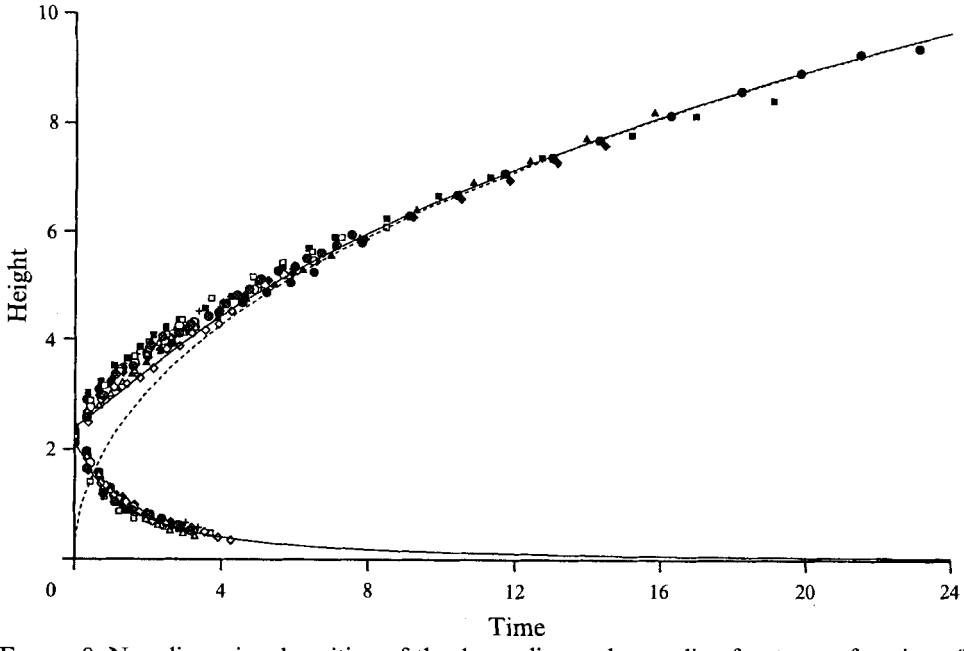

FIGURE 8. Non-dimensional position of the descending and ascending fronts as a function of time. The theoretical prediction for the former corresponds to the model described in §4.1. The position of the ascending front is predicted by the well-mixed model, with initial conditions (4.22) (dashed line), and (4.28) (solid line). The kinetic energy conversion efficiency, f, is 0.5.

D). We have for this reason presented the results of the numerical integration of (4.27*a*, *b*) with initial conditions (4.22*a*, *b*), for an average value of $N^2H/\Delta_0 = 0.066$. These results are compared with the experimental data in figure 8.

The agreement between the theoretical prediction and the experimental results is good for $\tau > 6$. The value of f required to give the best fit for each data set varies from 0.4 to 0.6. The variability of the experimental results can totally account for this range of f. Therefore, relating the work for entraining fluid across the density interface to the input of kinetic energy into the system by the simple argument described above (equation (4.16)) allows us to successfully model the experiments. The efficiency of conversion of the available kinetic energy into potential energy of the stratification is approximately 50%. Energy losses are due to viscous dissipation and internal wave radiation.

It is known that a plume rising in a linearly stratified environment spreads out at a level ζ_0 between 2.13 and 2.8 (Turner 1979). Our experimental results suggest that the top of the layer of fluid flowing out sideways lies close to 2.4 (see figure 8). Hence we may consider a different initial condition

$$\zeta_0 = \Delta\beta_0 = 2.4. \qquad (4.28a, b)$$

Physically, this means that all the environmental fluid below the initial spreading height is instantaneously mixed at $\tau = 0$. The solution for an ideal source will in this case be

$$\zeta = (\zeta_0^2 + 2^{\frac{4}{3}}(1+2f)\tau)^{\frac{1}{2}} \qquad (4.29a)$$

$$\Delta\beta = \left(\Delta\beta_0 - \frac{2f}{1+2f}\zeta_0\right)\left(\frac{\zeta}{\zeta_0}\right)^{-1-1/f} + \frac{2f}{1+2f}\zeta, \qquad (4.29b)$$

with $\zeta_0 = \Delta\beta_0 = 2.4$.

The corresponding results for our laboratory source, including the buoyancy correction, have also been plotted in figure 8. As expected, for large τ the solutions for the two different initial conditions tend to each other. Using the revised initial condition, the model appears to agree with the data for $\tau > 4$. At this time the descending front has reached the bottom surface (within 8%), and the assumption of a homogeneous bottom layer becomes valid.

Equations (4.23*a*) and (4.29*a*) constitute respectively lower and upper bounds for the mixed-layer depth from an ideal source at large times. Indeed, initial condition (4.18*a*, *b*) corresponds to a state of lowest potential energy for the layer of fluid below the spreading level of the plume; in this case it is zero, since the system begins without a bottom layer, i.e. $h_0 = 0$. The alternative initial condition considered, given by (4.28*a*, *b*), corresponds to the maximum possible potential energy of the stable layer of height $h_0 = 2.4H$. It represents an initial potential energy of $\frac{1}{4}N^2h_0^3A\rho_r$ in the region below the plume top (the reference density ρ_r is taken to be that at $h = 0$). The system actually starts up with the buoyant fluid being released at height h_0 and a linear stratification below; the potential energy of this layer is intermediate between the two values pointed out above, $\frac{1}{6}N^2h_0^3A\rho_r$.

We note that the energy argument given above does not take into account the actual stratification at the entrainment level, and therefore its effect on the plume behaviour, for small times. Initially there is no discontinuous density interface. Therefore the mixing at the spreading level of the plume will be greater, since the resistance is then smaller than our model predicts; we can see in figure 8 that, for $\tau < 4$, the model underestimates the rate of rise of the front, as expected. However, this initial transient does not affect the long-time behaviour.

5. Discussion

5.1. *The energetics of plume mixing in a stratified fluid*

We have seen that the mixing process induced by a plume rising in a stratified region which is laterally bounded will eventually lead to the development of a density interface. Entrainment of ambient fluid across this interface, from above and into the convecting bottom layer, is an important dynamical process occurring at the top of the plume.

The model presented in §4.2 is based on a simple energy argument, relating the conversion of local kinetic energy of the plume into potential energy of the entrained fluid. It is now interesting to analyse the evolution of the system in terms of the global energetics.

For large times the system consists basically of a homogeneous bottom layer through which a plume rises, impinging on the stratified buoyant environment above. A schematic of the energy transformations then occurring is given in figure 9. As the plume fluid rises, its relative potential energy is released. Part of this energy is used to advect the surrounding environmental fluid, while another fraction is converted into kinetic energy of the fluid now in the plume; some losses due to viscous dissipation will occur. At height h, the kinetic energy transported by the plume is $0.5\rho_r B_0 h$, as given by (4.14). During the penetration of the plume into the overlying stratified environment, a fraction f of this energy is used to entrain buoyant fluid into the bottom layer; this energy is stored essentially in the form of potential energy since the kinetic energy associated with the lateral outflow of plume fluid and advection in the mixed layer is very small. Viscous effects and internal non-breaking waves, which contribute little to the mixing, will inevitably originate some losses, and so f is smaller than 1.

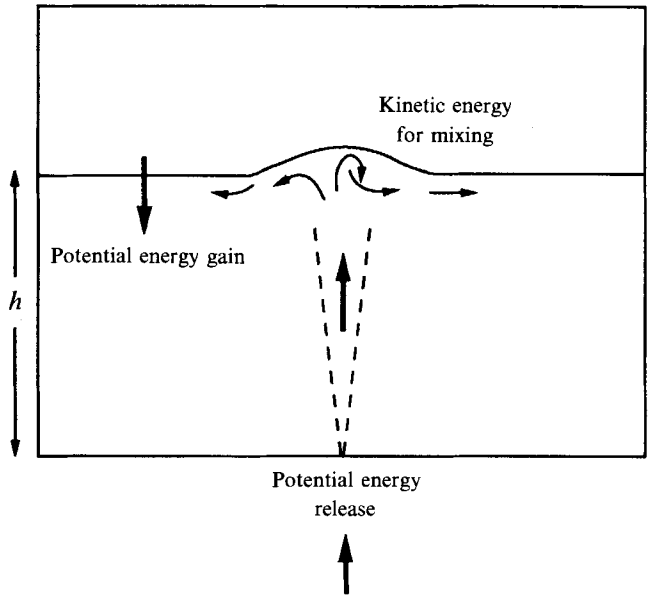

FIGURE 9. A schematic of the energy transformations occurring in the stratified filling-box process. Energy losses due to viscous dissipation and internal wave radiation occur throughout the mixed layer, particularly at the density interface at height h.

The change in potential energy associated with the development of a homogeneous density distribution in the mixed layer of depth h, from an initial linear distribution, is given by

$$\Delta E_{\mathrm{P}} = \rho_{\mathrm{r}} A(\Delta b \tfrac{1}{2}h^2 - \tfrac{1}{6}N^2h^3), \tag{5.1}$$

where Δb is the buoyancy difference at the interface. Since $h\Delta b = \frac{1}{2}N^2h^2 - (B_0/A)\,t$ (cf. (4.17)), this may be written as

$$\Delta E_{\mathrm{P}} = \tfrac{1}{2}\rho_{\mathrm{r}} Ah(\tfrac{1}{6}N^2h^2 - (B_0/A)\,t). \tag{5.2}$$

A schematic representation of the change in potential energy as a function of the height of the convective layer, h, for a fixed time t ($t > 0$), is shown in figure 10.

Let us begin by analysing the limiting situation for which ΔE_{p} is minimum. The evolution of the convective layer height will be given by

$$h_{\min} = (2(B_0/N^2A)\,t)^{\frac{1}{2}} \tag{5.3}$$

(in non-dimensional terms, $\zeta_{\min} = 2^{\frac{2}{3}}\tau^{\frac{1}{2}}$). Comparing this result with that obtained in §4.2, equation (4.23*a*), we see that it corresponds to the case in which $f = 0$. Hence, no kinetic energy is used for mixing; the interface is marginally stable, i.e. $\Delta b = 0$, and the mixed layer is encroaching upon, rather than entraining, the uniformly stratified layer above. A schematic vertical profile of buoyancy for this regime is depicted in figure 4(*a*).

When $\Delta E_{\mathrm{P}} = 0$, all kinetic energy supplied by the plume is converted into potential energy of the mixed layer, i.e. $f = 1$. This corresponds to the maximum entrainment intensity and is equivalent to Ball's limit (Ball 1960 and Manins & Turner 1978). The convective-layer depth is, in this case, described by

$$h_{\max} = (6(B_0/N^2A)\,t)^{\frac{1}{2}}. \tag{5.4}$$

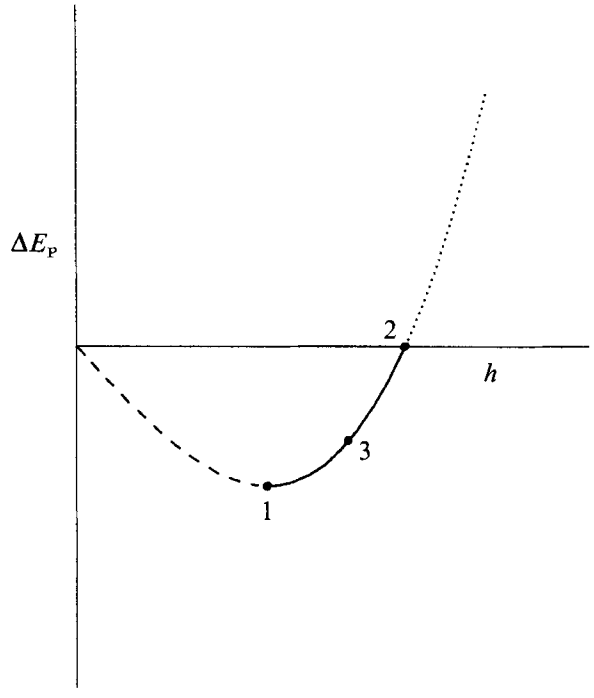

FIGURE 10. A schematic representation of the change in potential energy of the system as a function of the convective layer height, h, for a fixed time, t ($t > 0$). 1, Marginal convection, $f = 0$ (encroachment model); 2, maximum entrainment intensity, $f = 1$ (Ball limit); 3, observed, $f = 0.5$.

In this 'energy-conserving' limit, the convective layer depth is $\sqrt{3}$ times as great, at a given time, as when there is no entrainment. The buoyancy step at the top of the layer is now maximum, $\Delta b = \frac{1}{3}N^2h$.

Let us now consider the particular situation in which $f = 0.5$, as observed in our experiments. The convective-layer depth is intermediate between the two limits given above,

$$h_{\text{obs}} = (4(B_0/N^2A)\,t)^{\frac{1}{2}}. \tag{5.5}$$

The change in potential energy of the system is

$$\Delta E_P = -\frac{1}{24}\rho_r A N^2 h_{\text{obs}}^3, \tag{5.6}$$

corresponding to $1/\sqrt{2}$ of that in the marginal regime. During the course of convection the buoyancy profile in the mixed layer varies in a self-similar manner with $\Delta b = \frac{1}{4}N^2h$. This is because the efficiency of conversion of plume kinetic energy, f, is constant. We note that the change in potential energy is negative due to the injection of buoyancy into the system by the source.

The dashed part of the curve in figure 10 corresponds to unstable states in which $\Delta b < 0$; the dotted part represents global energy conversion efficiencies which cannot be achieved when mixing is performed by a plume. Indeed, the kinetic energy flux supplied by the plume to the top boundary of the mixed layer would have to be larger than the value given in (4.14) to obtain one of these states. This would imply a smaller fraction of the energy released by the buoyancy source being required for recirculation and viscous losses in the convective layer. In fact, in this sense a plume constitutes a

relatively efficient mixing agent. We shall see below that, for example, Rayleigh–Bérnard-type convection is a less efficient mixing mechanism and so the maximum change in potential energy of the system would in this case also be negative.

5.2. *The relation with turbulent penetrative convection: entrainment law*

At this stage it is useful to relate our results to those obtained in previous research on mixing by convective processes in stratified fluids. The problem of entrainment at the top of a convecting layer has usually been analysed in terms of the dependence of a dimensionless entrainment rate, E, given by

$$E = \frac{1}{\omega_*}\frac{\mathrm{d}h}{\mathrm{d}t}, \tag{5.7}$$

on the Richardson number, Ri,

$$Ri = a\Delta b/\omega_*^2. \tag{5.8}$$

Expressing the energy balance presented in §4.2 (equation (4.16)), in terms of these dimensionless variables, we have

$$E = c_1 \frac{\pi a^2}{A} Ri^{-1}, \tag{5.9}$$

where $c_1 = \frac{16}{5}\alpha f$; the velocity scale ω_* has been taken as the mean value over the cross-section of the plume at height h. The ratio of the active area of the interface to its total area appears in (5.9) due to the inherent localized mixing in our problem.

The functional relation derived above differs from the findings of both Linden (1973) and Baines (1975). The first author analysed the interaction of a vortex ring projected against a sharp density interface, while the latter considered the entrainment through the top of a plume (or jet) impinging on a density interface in a two-layered system. In both these works, an entrainment relation of the type $E \propto Ri^{-\frac{3}{2}}$ was observed. However, the experimental results presented in these papers are for large values of Ri, namely $Ri > 1$ and $Ri > 3$ respectively (a lengthscale equal to the radius of the mixing area is considered). In our experiments Ri evolved from approximately 0.2 (considering times sufficiently great for the well-mixed model to be valid) to 2.5. In fact, when analysing the tendency of Linden's data for the smaller values of Ri therein, a Ri^{-1} mixing law is observed. However, Linden did not comment upon this.

More recently, Kumagai (1984) extended the work of Baines (1975) to cover a broader range of values of the Richardson number, $0.1 < Ri < 70$. He presented an empirical entrainment law valid for this range of Ri. At large Ri, the asymptotic behaviour $E \propto Ri^{-\frac{3}{2}}$ was observed, while when $Ri \to 0$ the experimental results suggest a mixing law of the type $E =$ constant. Analysing the experimental results in figure 12 in Kumagai's paper, it is possible to model the results in an intermediate range of Ri, $1.2 < Ri < 30$, using a relation of the type $E \propto Ri^{-1}$ although this was not pointed out by the author. However, the range of Ri over which this law applies is somewhat larger than suggested by both the results of the previous investigations mentioned above, and those obtained in the present work.

Nevertheless, it seems that the apparently contrasting entrainment laws for the different regimes observed as Ri varies can be explained. According to Linden (1973), at large Ri, the entrainment process is controlled by the wave-like response of the interface to the bombardment of turbulent disturbances. The motion of the interface results in ejection of fluid from the undisturbed region and consequent mixing. This phenomenon was also observed by Kumagai (1984). However, at smaller Ri,

entrainment seems to be caused mainly by intrusions of large turbulent disturbances into the region of lighter fluid and the associated capture of small portions of this fluid.

In fact, the same functional variation has been reported in a number of laboratory experiments on penetrative convection and also in atmospheric and hydrospheric measurements. In these studies, the sources of buoyancy are distributed over the whole bottom surface; turbulence develops throughout the convecting layer and active mixing occurs over all the interface. Zilitinkevich (1991, pp. 1–77) has recently presented a comprehensive model which allows an explanation for the different entrainment regimes observed in these processes.

At this point it is interesting to give a quantitative comparison between our results and those previously published, including data on turbulent penetrative convection. However, it is difficult to define equivalent scales for velocity and length such that the Richardson number does represent adequately the dynamic conditions at the interface in these different processes.

We shall therefore analyse the different results in terms of the ratio of the buoyancy flux at the top of the convecting layer to that at the ground. This is an alternative formulation to that of $E(Ri)$. The buoyancy flux due to entrainment at the top of the mixed layer is given by

$$B_h = \Delta b \frac{\mathrm{d}h}{\mathrm{d}t} A. \tag{5.10}$$

The ratio B_h/B_0 represents the fraction of the energy released at the source, measured by the magnitude of B_0, which is converted into potential energy at the interface, measured by B_h. From §4.2, we have for a plume

$$B_h/B_0 = f. \tag{5.11}$$

According to our experimental results, $f = 0.5$, and the ratio of buoyancy fluxes is therefore equal to 0.5.

The results of Kumagai (1984) point to a maximum value for B_h/B_0 of approximately 0.2 (see his figure 13). This clearly suggests less efficient mixing than our results. The difference observed can partly be explained by significant stratification in the bottom layer. In a two-layered system, a time is eventually reached when the plume penetrates through the upper less-dense layer; this sets a limit on the time during which an experiment can be run. If this time is not sufficiently large for the bottom layer to have become almost homogeneous, then stratification in this layer is always important. Simple calculations suggest that Kumagai's experiments are in this regime. Thus, more energy is needed to overcome the greater resistance to mixing and a smaller value of B_h/B_0 should be obtained. We should also note that the buoyancy flux at the source, B_0, only represents the energy made available to the system in so far as the buoyancy in the environment can be considered constant. At large times, when the effect of the continuous increase of the environmental buoyancy becomes important, the relative buoyancy flux, B_{0_r}, is more appropriate (as discussed in §4.2). This can lead to an increase as high as 40% for the buoyancy flux ratio at small Ri (large times) in some of Kumagai's experimental results. However, the difference between our results and those of Kumagai seems to be too large to be entirely justified by these arguments.

Zilitinkevich (1991) has reviewed studies on turbulent penetrative convection and shows that the value of B_h/B_0 lies between 0.1 and 0.3, with a mean value of 0.2. When buoyancy is released over all the bottom surface, turbulence develops throughout the convecting layer. In contrast, the mixing produced by the plume is quite 'organized'; turbulent motion is restricted to the convecting fluid in the plume, while surrounding ambient fluid recirculates in a laminar state. Hence, energy 'losses' during the

transport from the bottom source to the top boundary where entrainment occurs, due to the convective motions in the mixed layer and inherent viscous dissipation, are greater in penetrative convection. We should therefore expect a higher value of B_h/B_0 in our experiments since here the energy released at the source is preferentially channelled to the upper boundary of the mixed layer through the plume. In this sense, a plume constitutes an efficient mixing agent. This result appears to support our findings.

Proceeding further, we can try to estimate the kinetic energy flux at the top boundary of the convecting layer for a distributed source of buoyancy. There appears to be no study of the turbulent velocity field developed in a neutral environment for the continuous release of buoyancy at such a source; we have therefore tentatively extrapolated the data of Deardorff & Willis (1985) for the vertical profiles of velocity in a linearly stratified system. It is found that

$$E_K \approx 0.27\rho_r \omega_*^3 A, \tag{5.12}$$

where

$$\omega_* = ((B_0/A)\, h)^{\frac{1}{3}}. \tag{5.13}$$

Hence,

$$E_K \approx 0.27\rho_r B_0 h. \tag{5.14}$$

This is smaller than the value obtained for a plume (cf. (4.14)), as expected. Taking into account this result and the mean value of $B_h/B_0 = 0.2$ for penetrative convection, suggested by Zilitinkevich (1991), we estimate an efficiency of 0.4 for the conversion of kinetic energy into potential energy at the interface. This value is similar to the value of f measured in our experiments.

5.3. *Two physical applications*

We shall now consider the quantitative application of the model developed in this paper to two different problems. The first illustration concerns the process of cooling of a room wherein thermal stratification is important; the convection pattern which arises when cooling is local and weak is described. We then consider a geological application: the replenishment of a magma chamber by the input of light new magma at the base.

5.3.1. *Cooling of a room at a top window*

Consider cooling of a stable, thermally stratified room 4 m high and 6 m wide as a result of heat transfer, from the warm interior to the cold exterior, through a small top window. We assume heat loss is sufficiently small that the descending convective plume of cold air initially spreads out at some intermediate level, H_{s_0}.

Suppose the surface area of the window is 0.1 m^2 and the difference in temperature between the interior and the exterior is 10 °C. The rate at which heat is transferred to the exterior, Q, is then of the order of 10 W (Holman 1983, pp. 265–304). The buoyancy flux due to cooling will be given by

$$B_0 = \beta g Q/\rho_r C_p, \tag{5.15}$$

where β is the thermal expansion coefficient and C_p is the specific heat capacity for air at constant pressure. Taking $\beta \sim \frac{1}{300}\mathrm{K}^{-1}$, $\rho_r \sim 10^{-3}$ g cm^{-3} and $C_p \sim 1$ J g^{-1} K^{-1}, we estimate a buoyancy flux of approximately 3×10^4 cm^4 s^{-3}. Consider a constant temperature gradient of 0.5 °C/m in the environment; the initial stratification is then linear, with a buoyancy frequency $N = 0.13$ s^{-1}. Under these conditions, the plume of cold air generated at the window will initially spread out at a level

$$H_{s_0} = 2.9 B_0^{\frac{1}{4}} N^{-\frac{3}{4}} = 1.8 \text{ m} \tag{5.16}$$

(this corresponds to $\zeta_0 = 2.13$, see §4.2). This distance is measured from the virtual origin of the plume, which can be shown to lie approximately 0.8 m above the window (see Morton *et al.* 1956).

Using (4.11), we can estimate the time needed for the top part of the room, from the window down to the spreading level, to become almost homogeneous in temperature. The position of the 'descending' front (§4.1) of mixed fluid, which moves towards the window is 0.8 m from the virtual source and we calculate a value for t of the order of 45 min. At this moment the actual depth of the mixed layer at the top of the room is approximately 1.8 m because the 'ascending' front has (§4.2) propagated a further 0.8 m down into the room from the initial spreading level, 1 m below the window (cf. (5.16)), calculated from (4.29*a*). As a result of the mixing action of the plume, warm air from the top of the room is transported down; somewhat counter-intuitively, during a transient period, the room then becomes warmer at the lower levels than if there were no cooling at its top. The increase in temperature may be determined from (4.29*b*); we estimate a temperature difference of approximately 0.4 °C between the mixed layer and the stratified environment immediately below.

The time required for the mixed air front to advance down to the ground can be calculated from (4.29*a*). In this case the 'ascending' front (§4.2) is 4.8 m below the virtual source, and we predict $t \sim 3$ h for this situation to be achieved. The room then has an almost uniform temperature, apart from the plume; it is 0.6 °C warmer at the floor level than expected without cooling. After this time, a front of cold air starts rising from the ground, analogous to the first front of Baines & Turner (1969).

It is interesting to mention that if one had assumed stratification in the room to be negligible and applied the theory of Baines & Turner (1969) for a uniform environment, the conclusions would be totally different. Then a cold air front would rise from the floor and the room would become gradually cooler from below; with stratification, this process would only occur after about 3 h.

Concluding this example, we should note that, due to the large area of the source, the displacement between real and virtual origins is a significant fraction of the total depth of the plume. The theory developed in §4 may then not be strictly valid; a real finite source should be considered. However, our purpose is to identify timescales for the different situations.

The conclusions above may be applied to the case of a noxious buoyant release in a closed space. Depending upon whether environmental stratification is dynamically important or not, totally different transient concentration distributions may ensue. This would be an important issue when deciding on the location and sensitivity of chemical and safety detectors necessary in a building; such an investigation would form an interesting extension to the present study.

5.3.2. *Replenishment of a magma chamber by a light input*

Magma chambers are often replenished by an influx of magma of density smaller than that of the resident magma (Huppert *et al.* 1986). For a continuous input of light magma, a turbulent plume may then rise above the source. If the resident magma is continuously stratified, this plume may penetrate only to some intermediate height in the chamber; it will then intrude horizontally. The dynamical evolution of the resulting mixing process may then be described by the model developed in §4.

Following Huppert *et al.* (1986), consider a magma of density 2650 kg m^{-3} to be input into the base of a chamber 1 km high. A steady flow rate in the range 1–100 m^3 s^{-1} is assumed. Let the stratification in the resident magma be linear, with a decrease in the density from 2700 kg m^{-3} at the base to 2660 kg m^{-3} at the roof. The

buoyancy flux at the source is then $B_0 = 0.18$–$18\ \mathrm{m^4\ s^{-3}}$ and the buoyancy frequency in the environment is $N = 1.2 \times 10^{-2}\ \mathrm{s^{-1}}$. The height at which the plume initially spreads out lies in the range $H_{s_0} = 50$–170 m, a small fraction of the total height of the chamber. (The coefficient in (5.16) is in accord with Turner 1986 and is different from that considered by Huppert *et al.*; hence our estimate for H_{s_0} is different.) We assume further that the magma chamber has a uniform cross-section, with area $A = 10^6\ \mathrm{m^2}$. Then, using (4.11), we predict that the descending front of mixed magma will reach the base of the chamber (within 10% of the initial spreading level) about 5–50 days after initiation of replenishment. An almost homogeneous convecting layer will then develop at the bottom of the chamber. Assuming a continual input of magma, the top boundary of this layer of mixed magma is then predicted to rise up to the roof of the chamber over a period of about 1–10 months (cf. (4.29)).

6. Conclusions

The fluid dynamics of buoyant convection in a stably stratified region of finite lateral extent has been investigated both experimentally and theoretically. We have restricted our analysis to the case of continuous convection from a point source of buoyancy; momentum and mass fluxes are assumed to be negligible. An initial linear density profile in the environment is considered.

As a result of the stratification, the rising turbulent plume in general penetrates only part way into the environment. In a region of large lateral extent (compared to the radius of the plume) it then intrudes sideways, forming a horizontal layer at an intermediate height. As time evolves, this layer of fluid, which has at some time been in the plume, increases in thickness. The bottom boundary descends due to the continual entrainment of surrounding ambient fluid into the plume. The process is analogous to that described by Baines & Turner (1969) for a uniform environment. It is also observed that the lateral spreading of the plume occurs at an ever-increasing level. This is a result of the evolution of the density field in the environment, and gives rise to an ascending top front. We present a theoretical model for this mixing process and predict the rate at which the two fronts advance into the environment.

We show that the effect of smooth stratification on the dynamics of the descending front is negligible. The rate at which this front travels is then well predicted by the theory of Baines & Turner (1969), with its position, h, relative to the source level, given by

$$h = H_{s_0}(1 + 0.11 H_{s_0}^{\frac{2}{3}} A^{-1} B_0^{\frac{1}{3}} t)^{-\frac{3}{2}}, \tag{6.1}$$

where time, t, is measured from the moment the plume first spreads out at height $H_{s_0} = 2.9 B_0^{\frac{1}{4}} N^{-\frac{3}{4}}$, B_0 is the buoyancy flux at the source, N is the buoyancy frequency in the original environment and A is the cross-sectional area of the region, assumed to be uniform. The rate of rise of the ascending front of plume fluid is shown to be determined by the turbulent mixing at the spreading level, caused by the collapse of the overshooting plume. Indeed, this results in significant entrainment of environmental fluid from above into the layer of plume fluid. An increasing density gradient then develops in this region – in the limit, a density jump occurs and the process of rise is therefore strongly restricted by this interface.

For sufficiently large times, when the descending front has practically reached the base of the region, the properties of the environment below the intruding level of the plume become almost homogeneous; a well-mixed layer can then be assumed. We present a model valid for these large times, based on a simple energetic argument. It

is proposed that a constant fraction of the kinetic energy of the plume at the interface level is used for mixing. The predictions of our model are in good agreement with the experimental results. These suggest that approximately 50% of the kinetic energy supplied by the plume for entraining fluid across the interface is converted into potential energy of the mixed layer. The interactive evolution of the convective layer depth, h, and the buoyancy step at the interface, Δb, is given by

$$h = H_{s_0}(1+0.23H_{s_0}^{\frac{2}{3}}A^{-1}B_0^{\frac{1}{3}}t)^{\frac{1}{2}}, \tag{6.2a}$$

$$\Delta b = 0.25N^2h, \tag{6.2b}$$

for $t > 20H_{s_0}^{-\frac{2}{3}}AB_0^{-\frac{1}{3}}$.

The energetic formulation presented is equivalent to assuming a turbulent entrainment law of the form $E \propto Ri^{-1}$, where E is the dimensionless entrainment coefficient (cf. (5.7)) and Ri is the Richardson number describing the dynamic conditions at the interface. Comparison of our results with previous studies on entrainment at a density interface, suggest that a relation of this type is only valid for an intermediate range of the Richardson number. At small Ri, the work of Kumagai (1984) suggests E = constant, while at large Ri his investigations and those of Linden (1973) and Baines (1975) point to a relation of the form $E \propto Ri^{-\frac{3}{2}}$. This functional variation is in accord with that reported in studies on turbulent penetrative convection.

We discuss the quantitative application of our model to the process of cooling of a room when stratification therein is relevant. It is shown that local weak cooling at the top can lead to transient warming at lower levels in the room. An increase in temperature of approximately 0.6 °C is estimated. The geological problem of replenishment of a magma chamber by a light input of molten rock is also analysed. We predict a timescale of the order of one month for mixing to extend throughout the chamber.

This work has been supported by the Commission of the European Communities Science Programme through grant B/910076. We would like to thank the anonymous reviewers for their very helpful comments.

Appendix A. Timescales of lateral outflow of plume fluid and of vertical advection

The model for the dynamics of the descending front, developed in §4.1, is valid if the lateral spreading of plume fluid occurs on a much smaller timescale than that of the vertical flow in the underlying environment; our assumption of instantaneous horizontal spreading is then a good approximation to the actual physical process. In this appendix, we derive conditions on the source strength and aspect ratio of the enclosed region required for the application of our model.

The lateral spreading of plume fluid is initially turbulent and this results in mixing with the overlying stratified fluid. However, this turbulence rapidly decays as it is suppressed by the stable stratification, and a high-Reynolds-number quasi-steady intrusion spreads radially from the plume axis. The dynamics of this outflowing current is then determined by a buoyancy–inertia balance and may be described by a Froude number

$$Fr = v/Nd, \tag{A 1}$$

where v denotes the velocity of the spreading current and d its thickness (see figure 11).

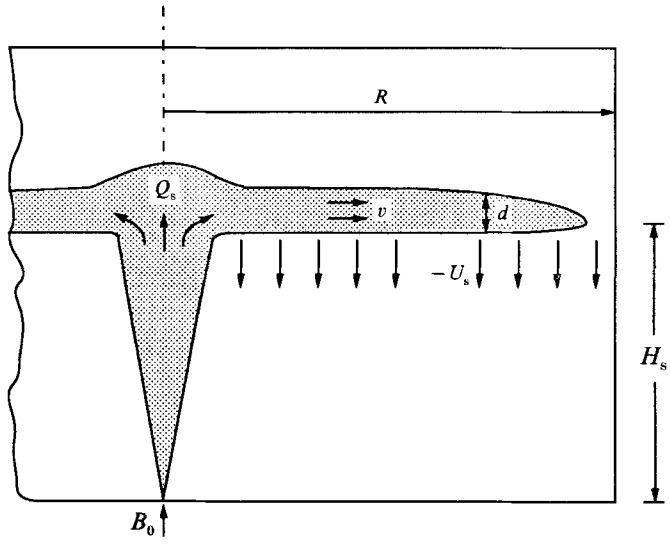

FIGURE 11. Sketch of the outflowing intrusion of plume fluid.

Following Manins (1979), we shall make the simplifying assumption that Fr is constant and equal to $\frac{1}{2}$. This is in fact a lower bound for Fr, since we are not taking into account the density jump which eventually develops at the spreading level in the environment (see §4.2). This simple analysis will therefore lead to an upper bound for the timescale of outflow.

We assume further that the downward velocity in the environment at the spreading level, U_s, is horizontally uniform; this is consistent with our experimental observations (see figure 2). Then, by continuity, the outward volume flux of the intrusion at radial position r is given by

$$Q = 2\pi r dv = Q_s + U_s \pi(r^2 - a_s^2), \qquad \text{(A 2}a, b\text{)}$$

where a_s is the plume radius at the spreading level and Q_s is the intrusion volume flux at $r = a_s$.

The radial dependence of d and v may be obtained from (A 1) and (A 2):

$$d = \left(\frac{Q_s}{2\pi r Fr N}\left(1 - \left(\frac{r}{R}\right)^2\right)\right)^{\frac{1}{2}}, \qquad \text{(A 3)}$$

$$v = \left(\frac{FrNQ_s}{2\pi r}\left(1 - \left(\frac{r}{R}\right)^2\right)\right)^{\frac{1}{2}}. \qquad \text{(A 4)}$$

The time for the outflow of fluid from $r = a_s$ to $r = R$ is then

$$t_1 = \int_{a_s}^{R} \frac{dr}{v} = 1.2\left(\frac{2\pi R^3}{FrNQ_s}\right)^{\frac{1}{2}}. \qquad \text{(A 5)}$$

Neglecting the small amount of fluid entrained as the plume impinges on the density interface, Q_s is the volume flux at height H_s of a plume rising in a uniform environment (see Turner 1979), and (C 5) may be written as

$$t_1 = 2.7(H_s^{-\frac{6}{3}} A^{\frac{3}{2}} B_0^{-\frac{1}{3}} N^{-1})^{\frac{1}{2}}. \qquad \text{(A 6)}$$

The timescale of vertical advection may be determined from the dynamics of the descending front, given by the rate of entrainment at the edge of the plume (cf. (4.11)).

The time taken for a front of plume fluid to descend to height $0.2H_s$, say, is approximately

$$t_2 = 20H_s^{-\frac{2}{3}} A B_0^{-\frac{1}{3}}. \tag{A 7}$$

Then

$$\frac{t_1}{t_2} = 0.14 \frac{B_0^{\frac{1}{6}}}{H_s^{\frac{1}{6}} A^{\frac{1}{4}} N^{\frac{1}{2}}}. \tag{A 8}$$

Hence, we may expect our assumption of instantaneous lateral spreading of plume fluid to be valid when this ratio is small. In our experiments, t_1/t_2 was typically 0.02.

Appendix B. The turbulent kinetic energy flux in a plume

In a recent extensive experimental investigation, Papanicolaou & List (1988) found that the r.m.s. turbulent fluctuations in velocity in plumes are self-similar and scale with the mean velocity. These authors have presented profiles of the intensity of turbulence fluctuations for the axial and radial velocity components. Using their results, the turbulent kinetic energy flux

$$E_{K_t} = \int_0^{+\infty} \rho \omega \tfrac{1}{2} (\overline{\omega'^2 + 2u'^2}) 2\pi r \, \mathrm{d}r \tag{B 1}$$

may be evaluated. Assuming a Boussinesq fluid, numerical integration leads to

$$E_{K_t} = 0.011 \rho_r \pi a^2 \omega^3 = 0.033 \rho_r B_0 h. \tag{B 2}$$

Comparing this result with that given in (4.14) shows that the kinetic energy flux associated with turbulence in a plume is small, less than 7% of that of the mean flow.

Appendix C. Change in potential energy of the mixed layer due to entrainment at the density interface

Consider an increase δh in the depth of the mixed layer during time interval δt. The change in potential energy is given by:

$$\delta E_P = \rho_r \Delta b h \delta h A - \rho_r \delta b (\tfrac{1}{2} h^2 + h \delta h) A, \tag{C 1}$$

while conservation of buoyancy requires, to leading order, that

$$\delta b = \delta h \Delta b / h. \tag{C 2}$$

Combining (C 1) and (C 2), leads to

$$\delta E_P = \rho_r \Delta b \tfrac{1}{2} h \delta h A. \tag{C 3}$$

The rate of change of potential energy of the mixed layer is then ($\delta t \to 0$)

$$\frac{\mathrm{d}E_P}{\mathrm{d}t} = \rho_r \Delta b \frac{h}{2} \frac{\mathrm{d}h}{\mathrm{d}t} A. \tag{C 4}$$

This result is equivalent to that given in §4.2, equation (4.15).

Appendix D. The inherent variability of our experimental results

The parameter $N^2 H / A_0$ varies from 0.053 in experiment 3A through to 0.083 in experiment 1A. The effect of this variation on the predicted height of the ascending front is shown in figure 12. The solid curve is the result for the mean value

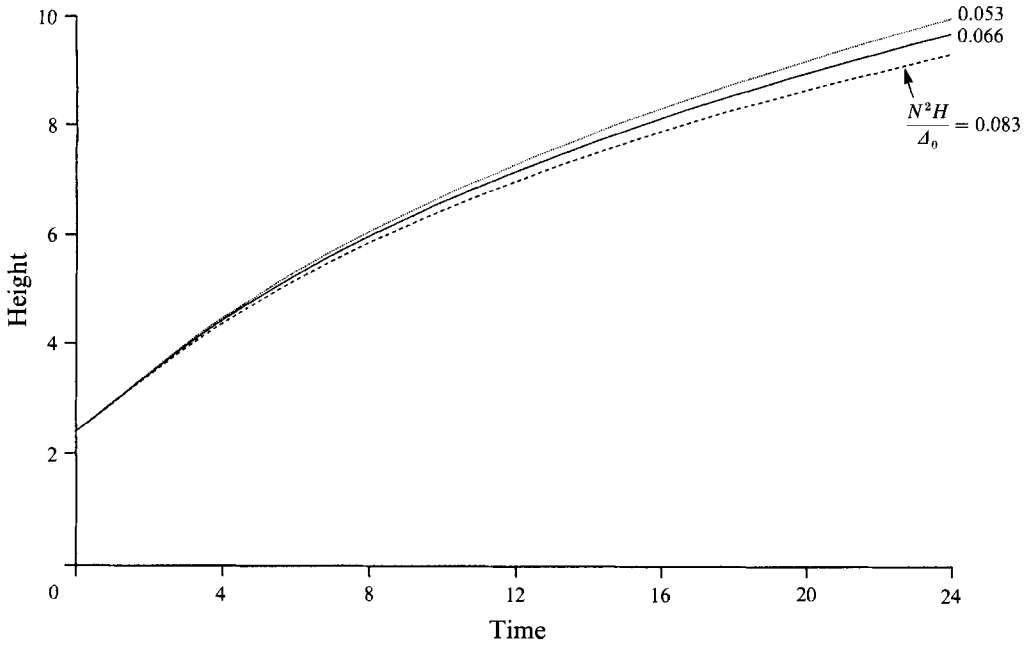

FIGURE 12. Effect of the parameter N^2H/Δ_0 on the predicted height of the ascending front.

$N^2H/\Delta_0 = 0.066$, considered in §4.2. The kinetic energy conversion efficiency has been taken as 0.5.

The difference seen in figure 12 cannot be resolved by our experimental results. Indeed, the inherent variability in these is of the same order of magnitude. The precision of our experimental results is mainly restricted by the difficulty in reading the position of the front of the shadowgraph. This interface is slightly irregular and more diffuse than one obtained in a system beginning with a finite discontinuity in density. The position of the front was determined to within ± 0.5 cm. The other important factor which leads to some scatter in the experimental results is the determination of the position of the virtual source (see §3). We estimate an error of ± 0.25 cm associated with this. The consequent variability in the experimental results restricts the accuracy with which we can predict the kinetic energy conversion efficiency, f.

In §4.2, we suggest that $f = 0.5 \pm 0.1$. Let us analyse the implication of this range in terms of the predicted position of the ascending front. In figure 13(*a*), we compare the data of experiment 1A with the theoretical prediction for $N^2H/\Delta_0 = 0.083$, the particular value for this experiment. Three curves are presented, for the mean and extreme values of f. It may be seen that close to $\tau = 6$, a value of f of 0.4 seems appropriate, while at $\tau = 12$, the experimental results suggest a value of 0.6. This difference is a result of inherent experimental error. A similar comparison is given in figure 13(*b*) for experiment 3A, with $N^2H/\Delta_0 = 0.053$.

Figure 13 shows that only longer experiments, i.e. larger τ than that covered in our study, could lead to a more precise estimation of f. This would require a larger tank than those used in our experiments, and an adequately sized system to produce the initial stratification. However, we should mention that our study seems to cover the conditions which are met in many physical situations, as shown by the examples in §5.3.

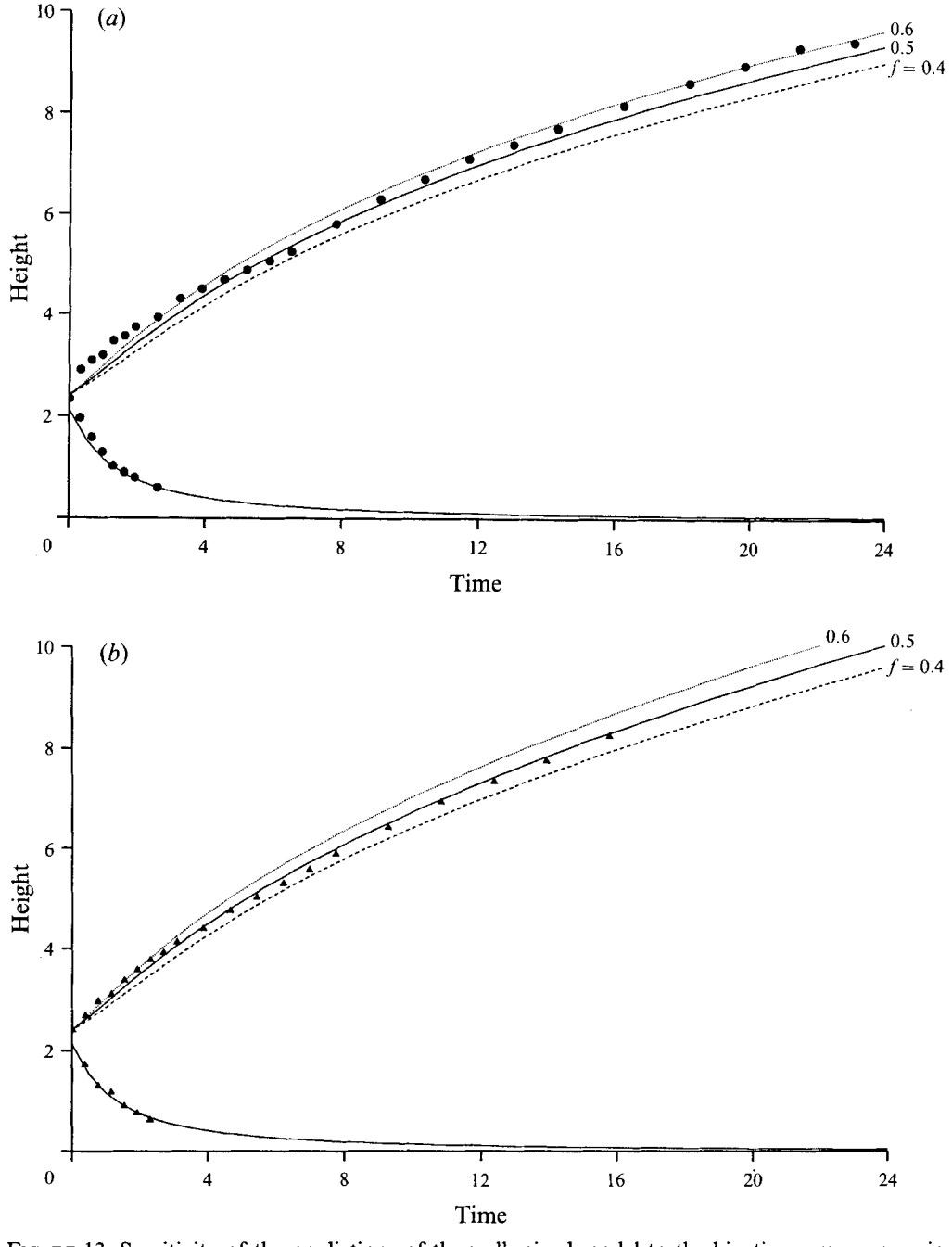

FIGURE 13. Sensitivity of the predictions of the well-mixed model to the kinetic energy conversion efficiency, f. Comparison of theoretical and experimental results for (*a*) experiment 1A and (*b*) experiment 3A.

REFERENCES

BAINES, W. D. 1975 Entrainment by a plume or jet at a density interface. *J. Fluid Mech.* **60**, 467–480.

BAINES, W. D. & TURNER, J. S. 1969 Turbulent buoyant convection from a source in a confined region. *J. Fluid Mech.* **37**, 51–80.

BAINES, W. D., TURNER, J. S. & CAMPBELL, I. H. 1990 Turbulent fountains in an open chamber. *J. Fluid Mech.* **212**, 557–592.

BALL, F. K. 1960 Control of inversion height by surface heating. *Q. J. R. Met. Soc.* **86**, 483–494.

BARNETT, S. J. 1991 The dynamics of buoyant releases in confined spaces. PhD thesis, University of Cambridge.

DEARDORFF, J. W. & WILLIS, G. E. 1985 Further results from a laboratory model of the convective planetary boundary layer. *Boundary-Layer Met.* **32**, 205–236.

GERMELES, A. E. 1975 Forced plumes and mixing of liquids in tanks. *J. Fluid Mech.* **71**, 601–623.

HOLMAN, J. P. 1983 *Heat Transfer*. McGraw Hill. pp. 265–304.

HUPPERT, H. E., SPARKS, R. S. J., WHITEHEAD, J. A. & HALLWORTH, M. A. 1986 Replenishment of magma chambers by light inputs. *J. Geophys. Res.* **91**, 6113–6122.

KUMAGAI, M. 1984 Turbulent buoyant convection from a source in a confined two-layered region. *J. Fluid Mech.* **147**, 105–131.

LINDEN, P. F. 1973 The interaction of a vortex ring with a sharp density interface: a model for turbulent entrainment. *J. Fluid Mech.* **60**, 467–480.

LINDEN, P. F. 1979 Mixing in stratified fluids. *Geophys. Astrophys. Fluid Dyn.* **13**, 3–23.

MANINS, R. C. 1979 Turbulent buoyant convection from a source in a confined region. *J. Fluid Mech.* **91**, 765–781.

MANINS, R. C. & TURNER, J. S. 1978 The relation between the flux ratio and the energy ratio in convectively mixed layers. *Q. J. R. Met. Soc.* **104**, 39–44.

MORTON, B., TAYLOR, G. I. & TURNER, J. S. 1956 Turbulent gravitational convection from maintained and instantaneous sources. *Proc. R. Soc. Lond.* A**234**, 1–23.

OSTER, G. 1965 Density gradients. *Sci. A.* **213**, 70–76.

PAPANICOLAOU, P. N. & LIST, E. J. 1988 Investigation of round vertical turbulent buoyant jets. *J. Fluid Mech.* **195**, 341–391.

TURNER, J. S. 1979 *Buoyancy Effects in Fluids*, pp. 165–206. Cambridge University Press.

TURNER, J. S. 1986 Turbulent entrainment: the development of the entrainment assumption, and its application to geophysical flows. *J. Fluid Mech.* **173**, 431–471.

WORSTER, M. G. & HUPPERT, H. E. 1983 Time-dependent density profiles in a filling box. *J. Fluid Mech.* **132**, 457–466.

ZILITINKEVICH, S. S. 1991 *Turbulent Penetrative Convection*. Avebury Technical.